J Therm Anal Calorim (2011) 105:93–99
DOI 10.1007/s10973-011-1641-3

Temperature dependent in situ doping of ALD ZnO

Zs. Baji · Z. Lábadi · Z. E. Horváth · M. Fried · B. Szentpáli · I. Bársony

Niinistö"s Special Chapter
© Akadémiai Kiadó, Budapest, Hungary 2011

Abstract This study on ALD grown ZnO layers is aimed at the systematic study of the effect of incorporation of different Al contents on the properties of the layers. An alternate precursor pulse method was used for layer deposition. Optimal doping was achieved at 210 °C at 2 at% Al content. A relationship between crystalline morphology versus temperature and aluminium incorporation was established.

Keywords Atomic layer deposition · Transparent conductive oxide · ZnO · Aluminium doping

Introduction

In most nanostructured thin film solar applications, there is a stringent need for the limitation of thermal budget. Recent advancement in polymer-based solar cells stresses this requirement even more, and restricts the maximum applicable temperature to <250 °C. This is another reason, why the usual Indium tin oxide (ITO) transparent conductive oxide (TCO) electrode is replaced by doped ZnO. This layer is preferably deposited by PVD methods, RF or reactive sputtering of an alloyed target. Another vacuum-compatible alternative could be the use of atomic layer deposition (ALD) of ZnO, especially when the requirements for conformality are essential, as in the case of, e.g. thin buffer layers. The adjustment of the conductivity of this TCO or buffer layer is, however, not obvious, since the introduction of sufficient amount of substitutional Al dopants into the ZnO matrix is a thermal budget limiting step as well.

The ALD is a self limiting layer growth method which consists of consecutive cycles of saturating surface reactions. The operation principle is based on a pulse-like introduction of precursor gases into the vacuum chamber, and their subsequent chemisorption on the heated substrate. Between the precursor pulses, the reactor is purged by an inert gas. Subsequently, the second precursor is introduced, and the reaction forms the conformal monolayer of the grown compound on the saturated surface. Under these circumstances the growth is stable, and the growth rate is constant [1–3].

TCOs are crucial for a number of applications, such as TFTs, solar cells, LEDs, field emitters, optoelectronic and electronic devices and transparent electronics. ZnO is a very popular TCO material because of its high melting point, chemical stability, direct band gap of 3.37 eV and high exciton binding energy (60 meV) [4]. In photovoltaic applications, ZnO is used as a buffer layer, or, when doped, as TCO.

The most widespread approach to increase the conductivity of ZnO is by doping with trivalent atoms, e.g. Al. This approach has made it possible to decrease the resistivity of sputtered layers to the minimum range of 10^{-4} Ω cm. [5] On the other hand, ALD ZnO films have an intrinsic resistivity of $\sim 10^{-2}$ Ω cm, also depending on a number of deposition parameters. This low value is believed to be the result of the presence of Zn interstitials, oxygen vacancies and hydrogen contamination [6, 7]. However, this resistivity can only be reduced by two orders of magnitude at the most by Al doping.

Between 100 and 200 °C growth temperature, the resistivity of intrinsic ZnO decreases monotonically.

Zs. Baji · Z. Lábadi (✉) · Z. E. Horváth · M. Fried · B. Szentpáli · I. Bársony
Research Institute for Technical Physics and Materials Science MFA, P.O. Box 49, 1525 Budapest, Hungary
e-mail: labadi@mfa.kfki.hu

Surprisingly, in this range both the electron mobility and the carrier concentration decrease at the same time, although generally increasing concentration is associated with decreasing mobility. The reason for this opposite effect in ALD ZnO may be the consequence of the improved crystal structure of the layers obtained at elevated deposition temperature [8–12].

According to the literature, the orientation of intrinsic ALD ZnO depends on the deposition temperature. According to [12, 13], the preferential orientation of the *c* axis changes from parallel to perpendicular to the substrate at increasing temperature, whilst the opposite conclusion may be drawn from [8, 9]. Epitaxial layer growth of ZnO was only reported on GaN [5, 14].

The effect of Al doping in the ALD process has not been studied extensively. It was reported that the lowest resistivity could be achieved with an Al content of 1.5–2 at%. At higher concentrations the mobility decreases, but the layers maintain their conductivity up to an Al concentration as high as 10 at%. Between 10 and 16 at%, the resistivity increases again, and small AlO_x grains are formed in the layers. The crystallinity of the doped ZnO deteriorates, they may even become amorphous. Although it was suggested that doping efficiency may correlate with the ALD growth temperature [15–18], so far no detailed investigation was conducted on the subject.

This study attempts to elucidate upon the above uncertainties in ALD ZnO growth.

Experimental

Doped and undoped ZnO layers were deposited in a Picosun SUNALE™ R-100 type ALD reactor. Diethylzinc (DEZn) precursor was used for the deposition of ZnO, and trimethyl-aluminium (TMAl) as source of Al dopant. The source of oxygen was in both cases H_2O vapour.

All precursors were electronic grade purity and kept at room temperature. The carrier gas and purging medium were 99.999% purity nitrogen. During deposition, the pressure in the chamber was 15 mbar. Flow rates of the precursor gases and water were 150 sccm. The pulse time of all precursors was 0.1 s, the purging times were 3 s after each metalorganic precursor pulse, and 4 s after the water pulses.

(100) Si wafers with 10–15 Ω cm resistivity and 3-mm thick soda lime glass were used as substrates. They were cleaned in cc.HNO_3 and high purity water.

One deposition cycle consisted of a DEZn or TMAl pulse, then a purge, followed by a water pulse, then a purge again. Using sequences of these cycles, the following Al–ZnO layers of different doping levels were prepared (Table 1).

Table 1 Deposition recipes for doped Al:ZnO layers

Deposition cycles	Atom%
500 layers ZnO	0
15 cycles of (30 layers ZnO + 1 layer AlO) + 30 layers ZnO	1.53
21 cycles of (21 layers ZnO + 1 layer AlO) + 21 layers ZnO	2.17
30 cycles of (15 layers ZnO + 1 layer AlO) + 15 layers ZnO	3.03
40 cycles of (11 layers ZnO + 1 layer AlO) + 11 layers ZnO	4.07
48 cycles of (9 layers ZnO + 1 layer AlO) + 9 layers ZnO	4.91

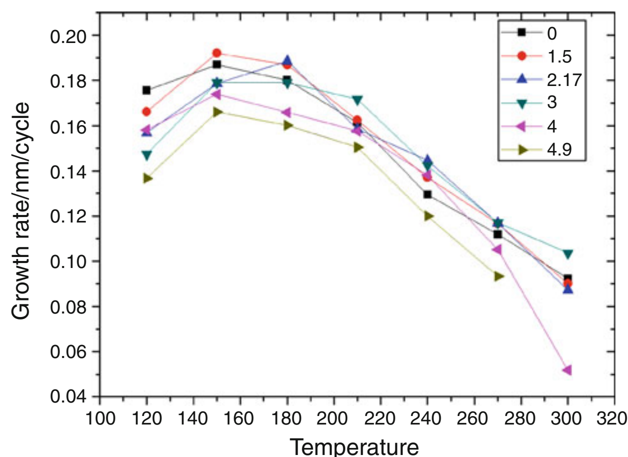

Fig. 1 Temperature dependence of the growth rate of Al:ZnO layers

The layers were deposited at seven different substrate temperatures between 120 and 300 °C. The 150 °C series consisted of samples with 12 different doping levels.

After the deposition, on the coated substrates of identical dimensions, electrical contacts were fabricated on the glass samples using silver paste. The sheet resistivities were measured in the Van der Pauw configuration. The thickness of the samples was determined by spectroscopic ellipsometry, and the respective spectra were evaluated with the Cauchy model. Crystal structure and orientation were examined by XRD using Philips PW 1050 diffractometer.

Results and discussion

Figure 1 shows the growth rates at different temperatures and different doping levels. The growth rate versus *T* curves have a maximum at around 150 °C, which corresponds to the location of the ZnO ALD window described in the literature [10]. The growth rate also correlates with the amount of the introduced Al, i.e. it decreases with increasing Al content. These general characteristics are similar at each growth temperature. The growth is slowing

down by increasing Al incorporation, since the AlO_x has to nucleate on ZnO surface and vice versa [16].

Figure 2 summarizes the specific resistivity of the layers as a function of the Al content and substrate temperature. We found that the aluminium incorporation up to a certain amount of Al content decreases the resistivity of zinc-oxide layers, and above that threshold value the resistivity starts to increase again.

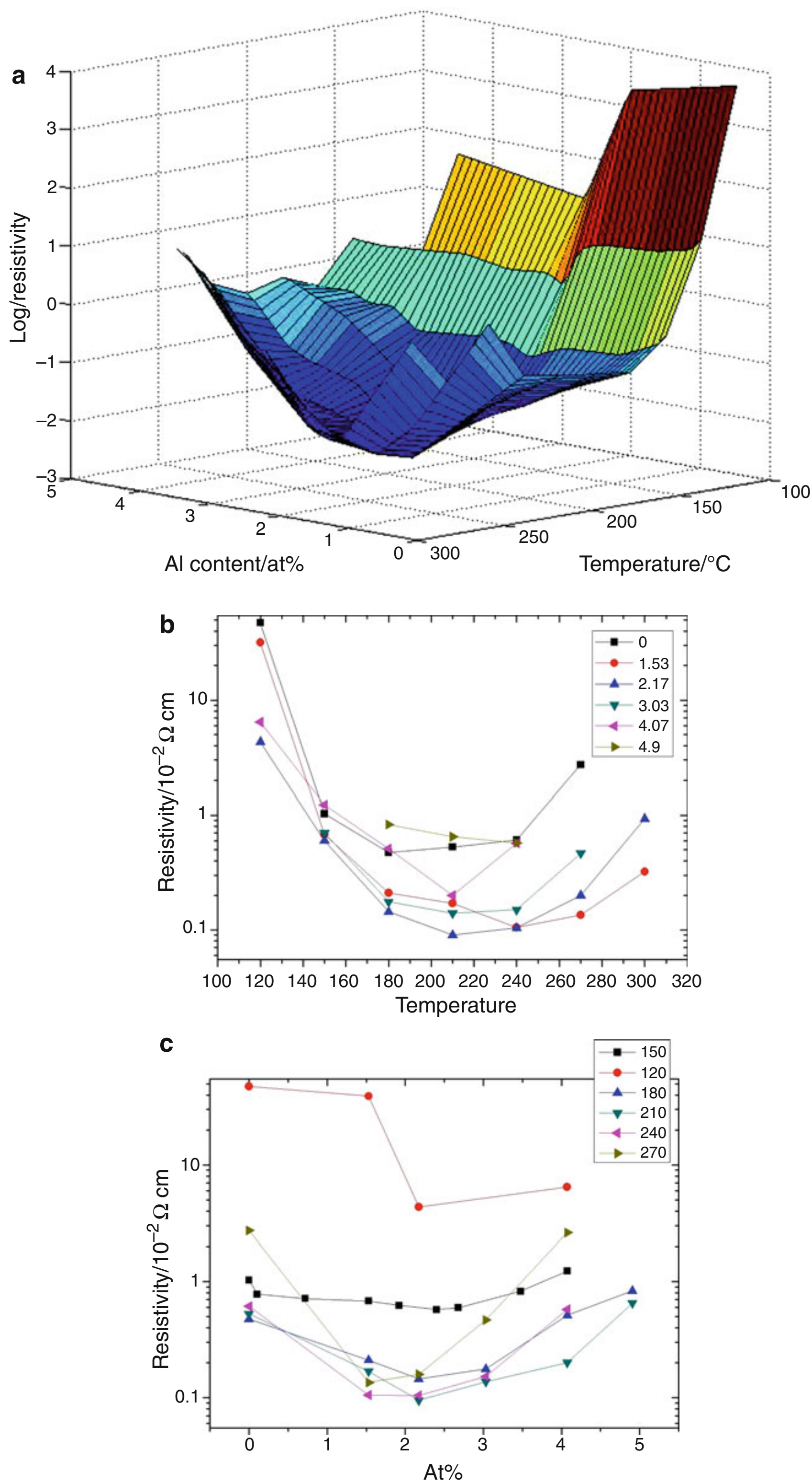

Fig. 2 Specific resistivity as a function of doping level and substrate temperature. **a** 3D view, **b** temperature dependence and **c** dependence on doping

The same experiment was repeated at six characteristic doping levels and six different deposition temperatures, so that the dependence of specific resistivity on both the temperature and the doping could be obtained. Our findings are shown in Fig. 2a, b, c. The two-dimensional surface in Fig. 2a shows the specific resistivity versus doping level and temperature, whilst Fig. 2b and c are projections of this surface.

The conductivity of the intrinsic ALD ZnO decreases between 120 and 210 °C in agreement with the literature data [9, 11, 12, 19]. The minimum of the intrinsic conductivity—as can be seen in Fig. 2b—is at 180 °C and its value is 4.7×10^{-3} Ω cm. Above 210 °C, the resistivity starts to increase again. As it can be seen in Fig. 2b, at a given level of doping the temperature dependence of the resistivity follows a "bathtub curve". All of these curves have their minimum around 210 °C. The doping effect increases with temperature (as proposed in [15–18]) up to this region, beyond this, the resistivity increases again. The doping has a maximum efficiency at around 210 °C.

Plotting the resistivity against aluminium concentration at a given temperature results a similar picture. Compared to the intrinsic value, the resistivity first drops then reaches its minimum at 1.5–2.5 at%, then at higher Al levels it increases rapidly again.

It can also be seen from Fig. 2, that the doping efficiency (i.e. the ratio of electrically active vs. incorporated Al) is also affected by the temperature.

To investigate the physical background of these changes in resistivity, we also performed Hall measurements. In Fig. 3a, we can see the mobility and the carrier concentration as a function of the deposition temperature in the case of the intrinsic samples. As opposed to [12], we found that the carrier concentration grows with the increasing deposition temperatures, then passing a maximum, in the same region where the resistivity has its minimum, and then it falls again. At the same time mobility decreases throughout the whole temperature range.

In Fig. 3b, the typical dependence of the mobility and the carrier concentration on aluminium content is shown for the 150° C series. The carrier concentration increases monotonically and the mobility decreases as a function of aluminium content. Although the aluminium incorporation occurs in a form of Al_2O_3 doping, a fraction of the Al proportional to the Al_2O_3/ZnO ratio is still incorporated as an electrically active dopant.

Figure 4 summarizes the XRD characterization results of our samples. Two characteristic SEM micrographs are also presented, reflecting the two preferential crystalline orientation in the ZnO layers. These are the (100), when the *c* axis of the ZnO unit cell is parallel with the substrate, and the (002), where the *c* axis is normal to the surface.

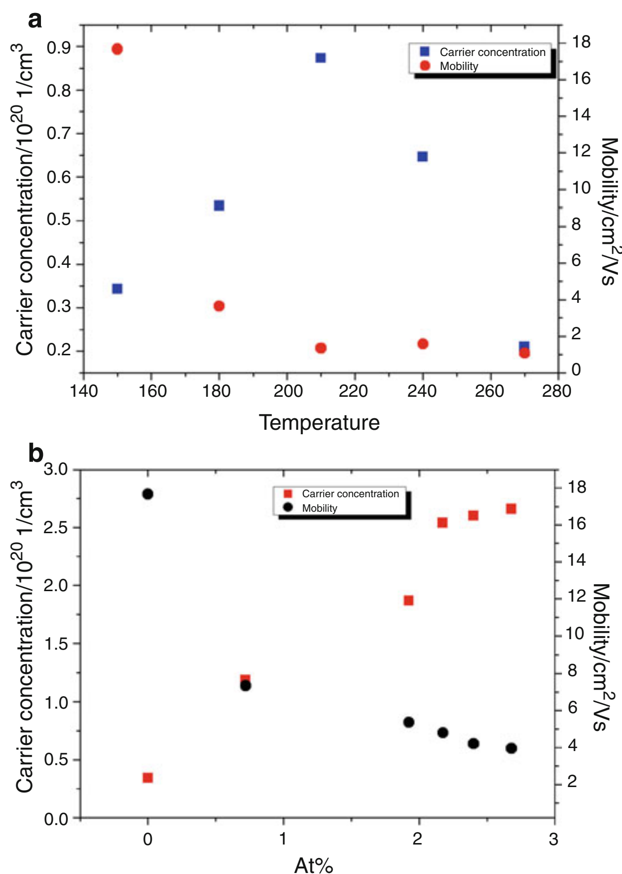

Fig. 3 Mobility and carrier concentration as a function of the deposition temperature (**a**) and concentration in the 150 series (**b**)

At every deposition temperature, the samples with the highest aluminium content of 5 at% and the intrinsic ones were analyzed and characterized in Table 2. The crystal structure is evidently influenced by the deposition temperature as well as by the doping level. All samples are comprised of polycrystalline ZnO, and no separate Al_2O_3 phase is visible. The samples deposited at higher temperatures have more pronounced crystallinity. The intrinsic ZnO grains have a dominant (100) orientation at 120 °C, that is, the *c* axis of the ZnO unit cell is parallel with the substrate. In the layers deposited at higher temperatures, the (002) orientation appears. In the sample prepared at 210 °C, both orientations are equally present. Above this temperature gradually the (002) orientation takes over, and in the layer deposited at 300 °C, the (002) orientation prevails. This trend is in agreement with the literature [12].

At the same time, the aluminium doping also plays a crucial role in determining the crystal structure and orientation. Al doping decreases the lattice constant at all temperatures (compressive strain), at higher temperatures this effect is more pronounced. The aluminium incorporation decreases the grain size and changes the preferred

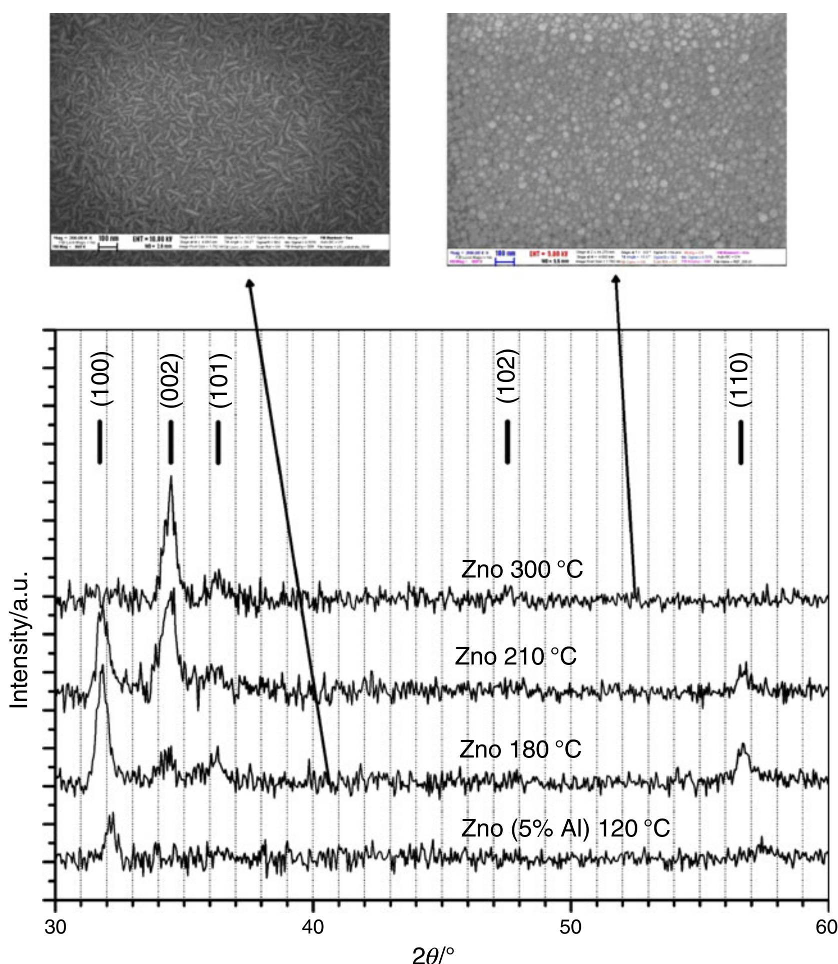

Fig. 4 XRD rocking curves of ALD ZnO layers deposited at different temperatures

Table 2 Summary of the XRD findings

	Intrinsic	4.9 at%
120°	Small grain size; typical orientation: (100)	No pronounced orientation, (100) apparent
150°	(100) dominant	No pronounced orientation, (100) apparent
180°	(100) orientation even more dominant	Beside the (100) orientation (101 appears)
210°	Besides (100) (002) becomes more apparent	(100) and (101)
240°	Better crystalline structure. (100) and (002)	No orientation, very small grains.
270°	(002) more dominant than (100) and (101), but all of them are present.	No orientation, very small grains.
300°	(002) orientation	No orientation, very small grains.

orientation. In the doped samples deposited at the lower temperatures, a (100) orientation is dominant, but not as much as in the undoped case. With increasing deposition temperature, in the intrinsic samples, the (002) orientation appears, whilst in the doped ones, the (101) orientation becomes apparent. Finally, at the highest deposition temperature, whilst in the intrinsic samples, the (002) orientation becomes dominant, in the aluminium doped ones, no preferred orientation can be detected, and the grain size becomes very small (which was also confirmed by the TEM analysis).

A summary of the XRD measurements can be seen in Table 2.

A spectroscopic ellipsometry study of our samples was also conducted using the Cauchy evaluation method, and thus we received refractive indices and thickness data of the layers at the same time.

Figure 5 shows the real part of the refractive index plotted against the atomic percent of the incorporated Al. All of the measured results from samples deposited at different temperatures follow a linear tendency within a narrow range. The refractive index decreases with

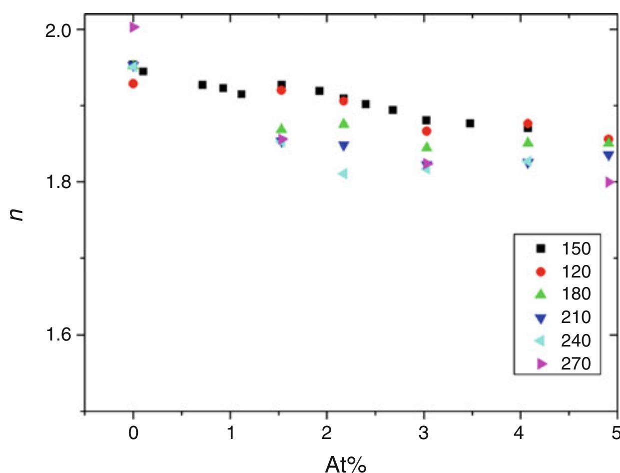

Fig. 5 Real part of the complex refractive index as a function of Al doping

aluminium incorporation, but does not depend on the deposition temperature. The refractive index of the intrinsic ZnO is in agreement with the literature data, whilst that of Al_2O_3 is 1.7. Therefore, we may say that with the incorporation of the aluminium, the refractive index of the layer is shifted towards that of Al_2O_3. The layers behave like a mixture of ZnO and Al_2O_3. As the XRD results reflect no phase separation, there are no Al_2O_3 grains present in the sample. The layers can thus be described as a homogeneous mixture, a solid solution.

Conclusions

We developed an ALD process for the in situ Al doping of ZnO. The procedure consists of periodic alternate injection of Al-precursor pulses intermixed with the sequences of Zn-precursor pulses. The specific resistances of the ALD Al:ZnO layers were evaluated as a function of the introduced atomic fraction of Al (i.e. number of Al-precursor pulses) and temperature. It was found that both the temperature and doping dependence of the resistivity develop a minimum: The optimal doping of the ALD deposited Al–ZnO is obtained around 2 at% at 210–240 °C substrate temperature.

Spectroscopic ellipsometry results show that the majority of aluminium is present in the form of Al_2O_3, however, not in a separate phase (as verified by XRD). The layers are rather homogenous mixtures of ZnO and Al_2O_3. The electrically active fraction of the Al content is sufficient to reduce the resistivity of the layers by two orders of magnitude.

The preferred crystalline orientation of the layers depends on the deposition temperature and the aluminium concentration as well. The aluminium incorporation reduces the grain size in the layers.

Acknowledgements The authors wish to thank the Hungarian National Science Fund OTKA (Grant No. NK 73424) for the support.

References

1. George SM. Atomic layer depositon: an overview. Chem Rev. 2010;110:111–31.
2. Ritala M, Leskela M. Atomic layer deposition. In: Nalwa HS, editor. Handbook of thin film materials. San Diego: Academic Press; 2001. p. 103–59.
3. Niskanen A, Hatanpää T, Ritala M, Leskelä M. Thermogravimetric study of volatile precursors for chemical thin film deposition: estimation of vapor pressures and source temperatures. J Therm Anal Calorim. 2001;64:955–64.
4. Wachinicki L, Kravewski T, Luka G, Witkowski B, Kowalski B, Kopalko K, Domagala JZ, Guziewicz M, Godlewski M, Guziewicz E. Monocrystalline zinc oxide films grown by atomic layer deposition. Thin Solid Films. 2010;518:4556–9.
5. Németh Á, Major Cs, Fried M, Lábadi Z, Bársony I. Spectroscopic ellipsometry study of transparent conductive ZnO layers for CIGS solar cell applications. Thin Solid Films. 2008; 516:7016–20.
6. Pearton SJ, Norton DP, Ip K, Heo TW, Steiner T. Recent progress in processing and properties of ZnO. Superlattices Microstruct. 2003;34:3–32.
7. Özgür Ü, Alivov Ya I, Liu C, Teke A, Reshchikov MA, Doğan S, Avrutin V, Cho S-J, Morkoç H. A comprehensive review of ZnO materials and devices. J Appl Phys. 2005;98:041301.
8. Lu JG, Ye ZZ, Zeng YJ, Zhu LP, Wang L, Yuan J, Zhao BH, Liang QL. Structural, optical, and electrical properties of (Zn, Al)O films over a wide range of compositions. J Appl Phys. 2006;100:073714.
9. Yamada A, Sang B, Konagai M. Atomic layer deposition of ZnO transparent conducting oxides. Appl Surf Sci. 1997;112:216–22.
10. Lim J, Lee C. Effects of substrate temperature on the microstructure and photoluminescence properties of ZnO thin films prepared by atomic layer deposition. Thin Solid Films. 2007;515:3335–8.
11. Lim SJ, Kwon S, Kim H. ZnO thin films prepared by atomic layer deposition and RF sputtering as an active layer for thin film transistor. Thin Solid Films. 2008;516:1523–8.
12. Godlewski M, Guziewicz E, Luka G, Krajewski T, Lukasiewicz M, Wachnicki L, Wachnicka A, Kopalko K, Sarem A, Dalati B. ZnO layers grown by Atomic Layer Deposition: a new material for transparent conductive oxide. Thin Solid Films. 2009;518:1145–8.
13. Wójcik A, Godlewski M, Guziewicz E, Minikayev R, Paszkowicz W. Controlling of preferential growth mode of ZnO thin films grown by atomic layer deposition. J Cryst Growth. 2008;310:284–9.
14. Chen HC, Chen MJ, Liu TC, Yang JR, Shiojiri M. Structure and stimulated emission of a high-quality zinc oxide epilayer grown by atomic layer deposition on the sapphire substrate. Thin Solid Films. 2010;519:536–40.
15. Kirby SD, van Dover RB. Improved conductivity of ZnO through codoping with In and Al. Thin Solid Films. 2009;517:1958–60.
16. Yousfi EB, Weinberger B, Donsanti F, Cowache P, Lincot D. Atomic layer deposition of zinc oxide and indium sulphide layers for Cu(In,Ga)Se2 thin-film solar cells. Thin Solid Films. 2001;387:29–32.
17. Ahn CH, Kim H, Cho HK. Deposition of Al doped ZnO layers with various electrical types by atomic layer deposition. Thin Solid Films. 2010;519:747–50.

18. Saarenpaa H, Niemi T, Tukiainen A, Lemmetyinen H, Tkachenko N. Aluminium doped zinc oxide films grown by atomic layer deposition for organic photovoltaic devices. Sol Energy Mater Sol Cells. 2010;94:1379–83.
19. Krajewski T, Guziewicz E, Godlewski M, Wachnicki L, Kovalik IA, Wojcik-Glodowska A, Lukasiewicz M, Kopalko K, Osinniy V, Guziewicz M. The influence of growth temperature and precursors' doses on electrical parameters of ZnO thin films grown by atomic layer deposition technique. Microelectron J. 2009;40:293–5.